REGULAR ARTICLE

blood advances

CD14$^+$/CD31$^+$ monocytes expanded by UM171 correct hemophilia A in zebrafish upon lentiviral gene transfer of factor VIII

Muhammad Elnaggar,[1,2,*] Anjud Al-Mohannadi,[1,*] Waseem Hasan,[1] Doua Abdelrahman,[1] Mohammed J. Al-Kubaisi,[1] Igor Pavlovski,[1] Giusy Gentilcore,[1] Abbirami Sathappan,[1] Dhanya Kizhakayil,[1] Aesha I. Ali,[1] Suruchi Mohan,[3] Damilola Olagunju,[3] Chiara Cugno,[1] Jean-Charles Grivel,[1] Chiara Borsotti,[4] Antonia Follenzi,[4,†] Sahar I. Da'as,[1,5,†] and Sara Deola[1,†]

[1]Research Department, Sidra Medicine, Doha, Qatar; [2]Division of Hematology and Medical Oncology, Icahn School of Medicine at Mount Sinai, New York, NY; [3]Department of Obstetrics and Gynecology, Sidra Medicine, Doha, Qatar; [4]Department of Health Sciences, Università degli Studi del Piemonte Orientale Amedeo Avogadro, Novara, Italy; and [5]College of Health and Life Sciences, Hamad Bin Khalifa University, Doha, Qatar

Key Points

- A flow cytometry–based blood screening revealed that HSC transmit native and lentiviral vector transgenic FVIII preferentially to CD14$^+$/CD31$^+$ monocytes.
- CD14$^+$/CD31$^+$ monocytes derived from FVIII-transduced HSC rescued the bleeding phenotype in a novel zebrafish model of hemophilia A.

Emerging gene therapy clinical trials test the correction of hemophilia A (HA) by replacing factor VIII (FVIII) in autologous hematopoietic stem cells (HSCs). Although it is known that platelets, monocyte/macrophages, and mesenchymal stromal cells can secrete transgenic FVIII, a systematic examination of blood lineages as extrahepatic sources of FVIII, to our knowledge, has not yet been performed. In this study, we sought to provide a comprehensive map of native and lentivirus-based transgenic FVIII production from HSC stage to mature blood cells, through a flow cytometry analysis. In addition, we generated a model of transient HA in zebrafish based on antisense RNA, to assess the corrective potential of the FVIII-transduced HSCs. We discovered that FVIII production begins at the CD34$^+$ progenitor stage after cytokine stimulation in culture. Among all mature white blood cells, monocytes are the largest producers of native FVIII and can maintain protein overexpression during differentiation from HSCs when transduced by a FVIII lentiviral vector. Moreover, the addition of the HSC self-renewal agonist UM171 to CD34$^+$ cells during transduction expanded a subpopulation of CD14$^+$/CD31$^+$ monocytes with excellent ability to carry the FVIII transgene, allowing the correction of HA phenotype in zebrafish. Finally, the HA zebrafish model showed that *f8* RNA is predominantly localized in the hematopoietic system at the larval stage, which indicates a potential contributory role of FVIII in hematopoiesis that warrants further investigation. We believe that this study may be of broad interest to hematologists and researchers striving to advance knowledge and permanent treatments for patients with HA.

Introduction

Hemophilia A (HA) is an X-linked monogenic bleeding disorder caused by dysfunction or deficiency of factor VIII (FVIII); HA affects ~800 000 individuals worldwide (World Federation of Hemophilia Annual Global Survey 2020 https://www1.wfh.org/publications/files/pdf-2045.pdf). The use of viral vectors

Submitted 23 September 2022; accepted 22 November 2022; prepublished online on *Blood Advances* First Edition 7 December 2022. https://doi.org/10.1182/bloodadvances.2022009014.

*M.E. and A.A.-M. contributed equally to this study.

†A.F., S. Da'as, and S. Deola contributed equally to this study.

Data are available on request from the corresponding author, Sara Deola (sdeola@sidra.org).

The full-text version of this article contains a data supplement.

delivering FVIII, such as adeno-associated viral vectors[1] and, more recently, lentiviral vectors (LVs), has been experimentally tested in an attempt to permanently correct HA.[2] Adeno-associated viral vector–mediated correction of liver hepatocytes was successful, reaching phase 3 clinical trials of gene therapy (GT) (www.clinicaltrials.gov, #NCT04370054 and #NCT04323098). However, several limitations, mainly related to preexisting immunity and chronic liver disease, narrow the inclusion criteria of patients with HA eligible for this therapy.[3] In addition, a decay of transduced hepatocytes, potentially caused by cell toxicity, has been reported.[4]

To circumvent these limitations, data from recent studies have suggested that CD34$^+$ hematopoietic stem cells (HSCs) could be a potential source of GT in HA (www.clinicaltrials.gov; #NCT05265767, #NCT03217032, and #NCT03818763).[5] The scientific basis for these studies is formed by evidence of extrahepatic FVIII sources, such as bone marrow,[6] HSC-derived platelets,[7,8] monocytes/macrophages,[9,10] and mesenchymal stromal cells.[11] However, there is no comprehensive understanding of extrahepatic production and storage of FVIII in humans.

In this study, we sought to characterize the ability of HSC and their cell progeny to produce FVIII, and to identify optimal candidates for HA GT among mature blood lineages. We based our screening on the flow cytometry (FC) method developed for intracellular detection of FVIII in blood cells.[12] We selected the candidate cells best suited to carry FVIII transgene and we validated their therapeutic FVIII production capacity in an *f8* knockdown zebrafish (ZF; *Danio rerio*) model.

Methods

Isolation of CB-derived CD34$^+$ cells

Cord blood (CB) samples were collected from healthy donors after informed consent (Sidra Institutional Review Board, #1500788). CD34$^+$ cells were selected after Ficoll gradient separation and miniMACS immune selection (Miltenyi Biotec). CD34$^+$ cell purity was regularly checked after selection and usually reached 80%.

Prestimulation and LV transduction of CD34$^+$ cells

Cells were seeded in 96-well plates at 150 × 10^3 per well, prestimulated for 24 hours with thrombopoietin 100 ng/mL, stem cell factor (SCF) 300 ng/mL, Flt3-L 300 ng/mL, and interleukin 3 60 ng/mL[12] (hereinafter HSC-cytokine medium) with or without 38 nM UM171 (a pyrimidoindole derivative) and single hit transduced with LV-hPGK-hBDDFVIII[13] or LV-hPGK-GFP and rLV.EF1.tdTomato-9 (Takara Bio) with variable multiplicity of infection (MOI) for 16 to 18 hours. After transduction, cells were washed to remove the residual vector. Subsequently, they were either further cultured in HSC-cytokine medium with or without UM171 for FC assessments or sorting or immediately placed in the colony-forming unit (CFU) assay or differentiation cultures together with their untransduced counterparts. UM171 was replaced every 2 days.

FC staining

FC staining was performed with anti-CD34, anti-CD38 anti-CD45, anti-CD19, anti-CD4, anti-CD8, anti-CD3, anti-CD14, anti-CD31, anti-EPCR/CD201, anti-CD45RA, and anti-CD10 antibodies (BioLegend). Unlabeled anti-FVIII antibodies GMA-8024 (Green Mountain Antibodies) and matched immunoglobulin G isotype controls (Southern Biotec) were labeled using Zenon technology (Invitrogen) for intracellular FVIII staining according to the protocol described elsewhere.[14] Live/dead fixable staining was performed using the Zombie UV viability kit (BioLegend).

CFU assay

Cells were seeded in humidified 6-well plates at 700 cells per well in 2 mL MethoCult methylcellulose-based medium (STEMCELL Technologies). After 14 days, clonogenicity was assessed by counting colonies manually.

Myeloid cell/monocyte differentiation assay

Cells were seeded in 96-well plates at a 20 000 cells per well in 200 µL of cytokine-enriched medium and differentiated into monocytes in a 14-day culture (7-day expansion cycle with SCF/thrombopoietin/Flt-3L and 7-day differentiation cycle with SCF/Flt-3L/interleukin 3/macrophage colony–stimulating factor).[15]

Endothelial progenitor and cell differentiation assay

Cells were differentiated for 14 days in fibronectin-coated (Fibronectin protein, R&D Systems) 24-well plates at 2 million cells per mL in an endothelial differentiating medium, containing Iscove modified Dulbecco medium with 20% fetal bovine serum and cytokine stem cell growth factor 100 ng/mL and vascular endothelial growth factor 50 ng/mL (R&D Systems).[16]

CD45$^+$/CD31$^+$/CD14$^+$ cell sorting

CD34$^+$ transduced and untransduced cells were cultured for 10 days in HSC-cytokine medium + UM171, stained with anti-CD31, anti-CD14, and anti-CD45 antibodies, and then sorted for CD45$^+$/CD31$^+$/CD14$^+$ cells using the FACSAria Fusion Cell Sorter (BD Biosciences).

ZF models

Experiments using the ZF models were conducted under the institutional animal care and use committee protocol #EGFP2020-1138. Wild-type AB and transgenic fluorescent ZF Tg:gata1:dsRed-expressing red blood cells or Tg(fli1:EGFP)y[1] expressing enhanced GFP throughout the entire vasculature, were used for various experiments as indicated.

ZF xenotransplantation

ZF embryos were dechorionated 48 hours postfertilization, anesthetized with 0.08 mg/mL tricaine (MS-222, Western Chemical), and aligned in a 2% agarose (A9539, Sigma) microinjection plate in a petri dish.[17] CD34$^+$ cells (10 000 cells per µL) were loaded using needles (3-000-203-G/X, Drummond Scientific) and injected into the duct of Cuvier. Three hours after injection, ZF larvae were screened using a Zeiss LUMAR.V12 fluorescence stereomicroscope to select only successfully engrafted ZF for further analyses.

ZF dissociation for FC

The dissociation of ZF larvae to a single-cell suspension was performed after injection with LV-hPGK-GFP–transduced CD34$^+$ cells in accordance with a previously described protocol.[18] Single cells were then labeled for CD34 antigen before fluorescence-activated cell sorting acquisition.

MO-mediated knockdown

The ZF F8 protein shares 30.5% identity (51.3% similarity) in a 2361 amino acid overlap with human FVIII. The morpholino oligomer (MO) sequence, which blocks protein translation, was designed to knock down the expression of endogenous F8. A standard control MO (Control-MO, Gene Tools) was used as a negative control. The MO sequences were as follows: 5′-TTTACAATATCCTCA-CTCACTGTGC-3′ (f8-MO) and 5′-CCTCTTACCTCAGTTA-CAATTTATA-3′ (Control-MO). ZF were microinjected with MO diluted to concentrations of 0.5, 0.75, and 1.00 mM at the 1-cell stage or at 48 hours after fertilization using a PLI-100 Picolitre injector (Harvard Apparatus), as previously described.[19]

Laser-induced endothelial injury in ZF larvae

Laser-induced endothelial injury was performed on the caudal vein plexus (CVP) of ZF larvae on the first and second days after the injection, as previously described.[20] Using ZEISS PALM MicroBeam for laser microdissection, the endothelium of the CVP in the caudal area was targeted and ablated using 70% energy, 15 laser pressure catapulting, and 50% speed pulse for the measurement of clot formation time. Danioscope software (Noldus Technologies) was used to evaluate blood flow activity (measured in percentage) by measuring the change in pixel intensity in a selected area of interest in the dorsal aorta (DA) and posterior caudal vein (PCV) of the ZF.

Data analysis

FC analyses were performed using Kaluza (Beckman Coulter) and FlowJo (Becton Dickinson) software. All data representing FVIII were calculated after subtracting the relative immunoglobulin G. ZF images were analyzed using ZEN software (Zeiss), and cell mass size measurements were acquired using Danioscope. Descriptive and inferential (ie, *t* test and 1-way analysis of variance) statistical analyses were performed using GraphPad Prism.

Results

$CD34^+$ cells produce FVIII upon cytokine-induced differentiation in culture

To determine the blood cell subtype most suited for HA GT, we measured FVIII basal content in fresh or freshly thawed CB HSCs and their myeloid and lymphoid progenitor compartments. Total $CD34^+$ cells and myeloid and lymphoid progenitors expressed negligible amounts of FVIII, both when fresh and upon thawing. On average, $CD34^+$ HSCs expressed 0.44% (±0.2%) FVIII; $CD34^+$/$CD38^+$ common myeloid progenitors and $CD34^+$/$CD38^+$/$CD45RA^+$ granulocyte-monocyte progenitors expressed 0.33% (±0.3%) and 0.49% (±0.4%) FVIII, respectively. FVIII expression by $CD34^+CD10^+$ common lymphoid progenitors was 0.63% (±0.6%) (Figure 1A-B). In contrast, when $CD34^+$ cells were cultured, they became capable of de novo FVIII production. After 7 to 10 days of culture, CB $CD34^+$ FVIII expression increased to 12.18% (±9.4%) (Figure 1C-D).

Myeloid compartment of PBMCs is the main FVIII reservoir in the hematopoietic system

Next, to understand which lineage was most suitable for the expression of the FVIII transgene, we evaluated the intracellular content of FVIII in mature peripheral blood mononuclear cells (PBMCs) as direct evidence of the ability of cells to express FVIII. Bulk PBMC displayed an average of 2.3% (±1.3%) $FVIII^+$ cells (Figure 2A,C). Myeloid mononuclear cells showed the highest expression of FVIII among PBMCs (Figure 2C). CD11b cells showed 7.4% (±3.5%) $FVIII^+$ cells. The lymphoid compartment represented by $CD3^+$ T and $CD19^+$ B cells showed a relatively smaller contribution to the intracellular FVIII content, corresponding to 2.5% (±1%) and 1.5% (±1.2%) $FVIII^+$ cells, respectively.

$CD34^+$ cells overexpress FVIII after LV transduction

Subsequently, we sought to test to what extent $CD34^+$ HSCs could sustain FVIII protein expression. Therefore, we overexpressed FVIII by transducing CB $CD34^+$ cells with an LV, carrying a β-domain–deleted FVIII gene under the control of a phosphoglycerate kinase promoter (LV-hPGK-hBDDFVIII). Transductions were performed with an overnight single hit at increasing MOI titers: 50, 100, and 200 with a serum-free protocol, suited for $CD34^+$-mediated clinical GT.[12]

FC analyses to determine the expression of FVIII were performed 5 to 7 days after the transduction to eliminate false overexpression by transient nonintegrated DNA viral particles. Increasing MOIs resulted in a significant increase in $FVIII^+$ cells (14.6% ± 3.8%, $P = .049$) at 100 MOI transduction (Figure 3A-B). We showed in our previous work the ability of $CD34^+$ cells to actively secrete the overexpressed FVIII protein in the culture media using sensitive enzyme-linked immunosorbent assay (AlphaLISA).[14]

UM171 improves FVIII LV transduction

Next, we aimed to exploit the effect of adding the pyrimidoindole derivative UM171, an HSC self-renewal agonist[21] that is currently being tested in clinical trials for in vitro CB HSC expansion before allogeneic transplantation.[22,23] In our experiments, UM171 improved FVIII transduction with the highest peak at 20.3% ± 2.6% ($P = .027$) at 100 MOI. It significantly increased the yield of $CD34^+$ transduced cells (Figure 3C-D) while maintaining their safe clonogenic capacity, as confirmed via the CFU assay (Figure 3E).

These results from $CD34^+$ cells and PBMCs support the solid rationale for using $CD34^+$ cells as a GT target and stimulating the expression of FVIII protein in a mature lineage naturally prepared for the production of this protein. Based on our data and the evidence from the literature,[9,10] myeloid lineages exhibit the highest rate of $FVIII^+$ cells within PBMCs.

UM171 enriches a CD34-derived $CD14^+$/$CD31^+$ monocyte subset with high FVIII expression capacity

In addition, we assessed the persistence of FVIII expression throughout the maturation path of $CD34^+$ cells, focusing on the differentiation of the myeloid compartment as the richest lineage in FVIII. We cultured $CD34^+$ cells using a myeloid long-term culture (LTC) assay optimized for monocyte differentiation and expansion.[15] After monocyte-LTC, we achieved a distinct $CD14^+$/$CD33^+$ monocyte cell progeny that successfully showed the FVIII transgene expression in up to 7.9% ± 1.8% cells compared with the natural FVIII expression in 3.1% ± 1.3% untransduced cells ($P = .02$) (Figure 4A-B).

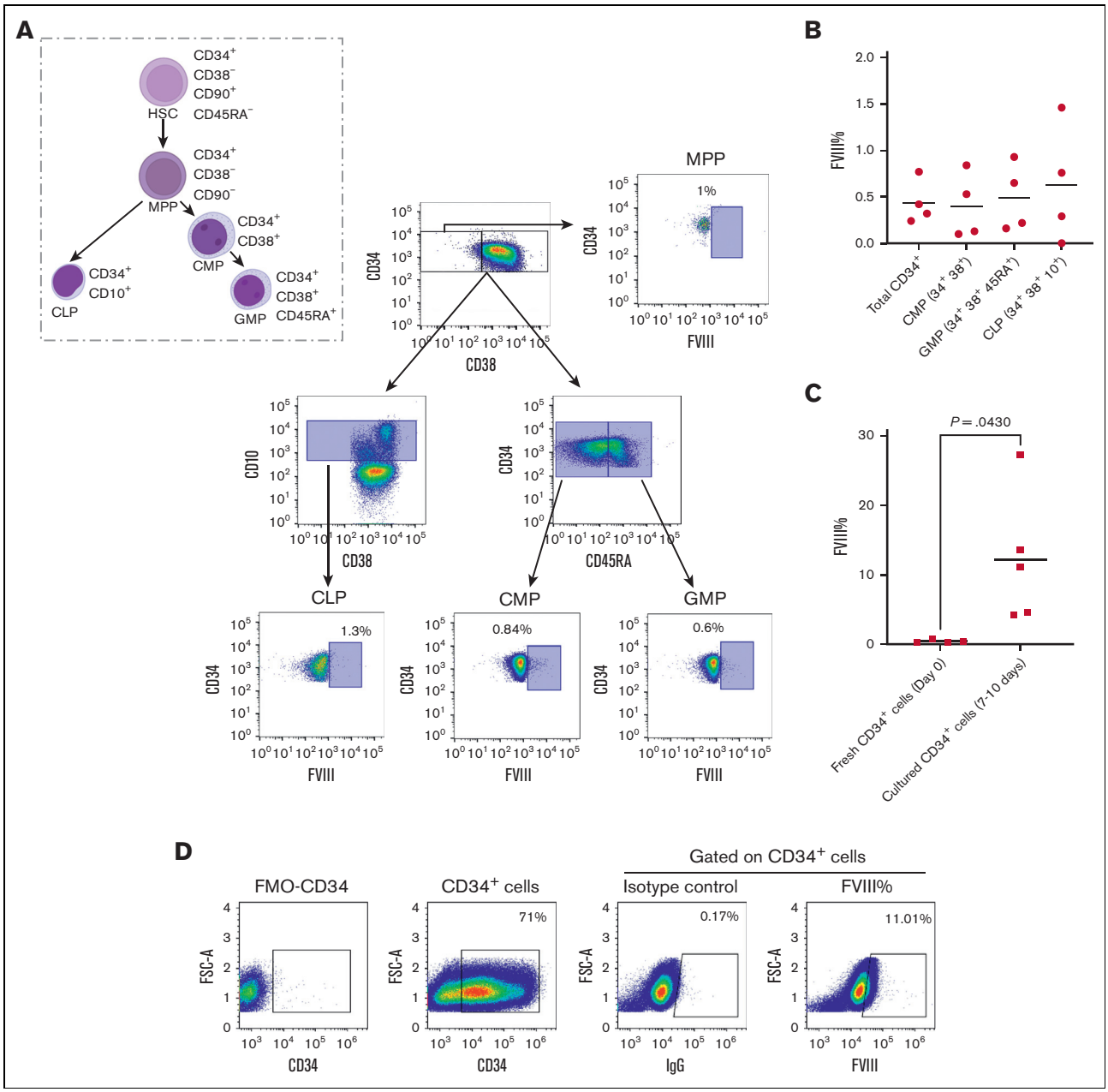

Figure 1. CD34$^+$ cells exhibit natural production of FVIII upon cytokine-induced differentiation in culture. (A-B) FVIII percentage in fresh human CB-derived CD34$^+$ HSCs measured as MFI by FC. (A) FC gating strategy and examples of FVIII percentage in different HSC progenitors. (B) FVIII percentage in total CD34$^+$ cells and different progenitors (n = 4, mean). (C) FVIII percentage in fresh vs cultured CD34$^+$ cells in serum-free medium (n ≥ 4, mean). (D) Representative FC plot of 7 to 10 days cultured CD34$^+$ cells. CLP, common lymphoid progenitor; CMP, common myeloid progenitors; FSC, forward scatter; GMP, granulocyte-macrophage progenitor; IgG, immunoglobulin G; MFI, mean fluorescence intensity; MPP, multipotent progenitor.

Seminal literature has described that bone marrow–derived mononuclear cells may generate endothelium.[24] Moreover, it has previously been shown how monocytes could acquire endothelial properties under angiogenic conditions.[25,26] FVIII is naturally produced and stored in endothelial cells,[27] thus, the expression of the FVIII transgene in endothelial cells would ensure the physiological production of this protein in the human body. Therefore, we assessed the capacity of CD34$^+$ FVIII–transduced cells to maintain the transgene after endothelial differentiation assay (e-LTC).[28]

We failed to observe classical CD45$^-$/CD144$^+$(VE-Cadherin)/CD202b$^+$(Tie2) mature endothelial cells after e-LTC (data not shown). Nevertheless, a large number of cells in the endothelial-driving milieu were characterized by an adherent and elongated spindle shape (Figure 4C, left panel), which suggested skewing toward endothelium differentiation.[28] By phenotyping these cells after the assay, we found the enrichment of CD45$^+$/CD14$^+$ monocytes upregulating the CD31$^+$ (PECAM-1) endothelial antigen, a vascular antigen with transmigratory ability.[29] In parallel, the

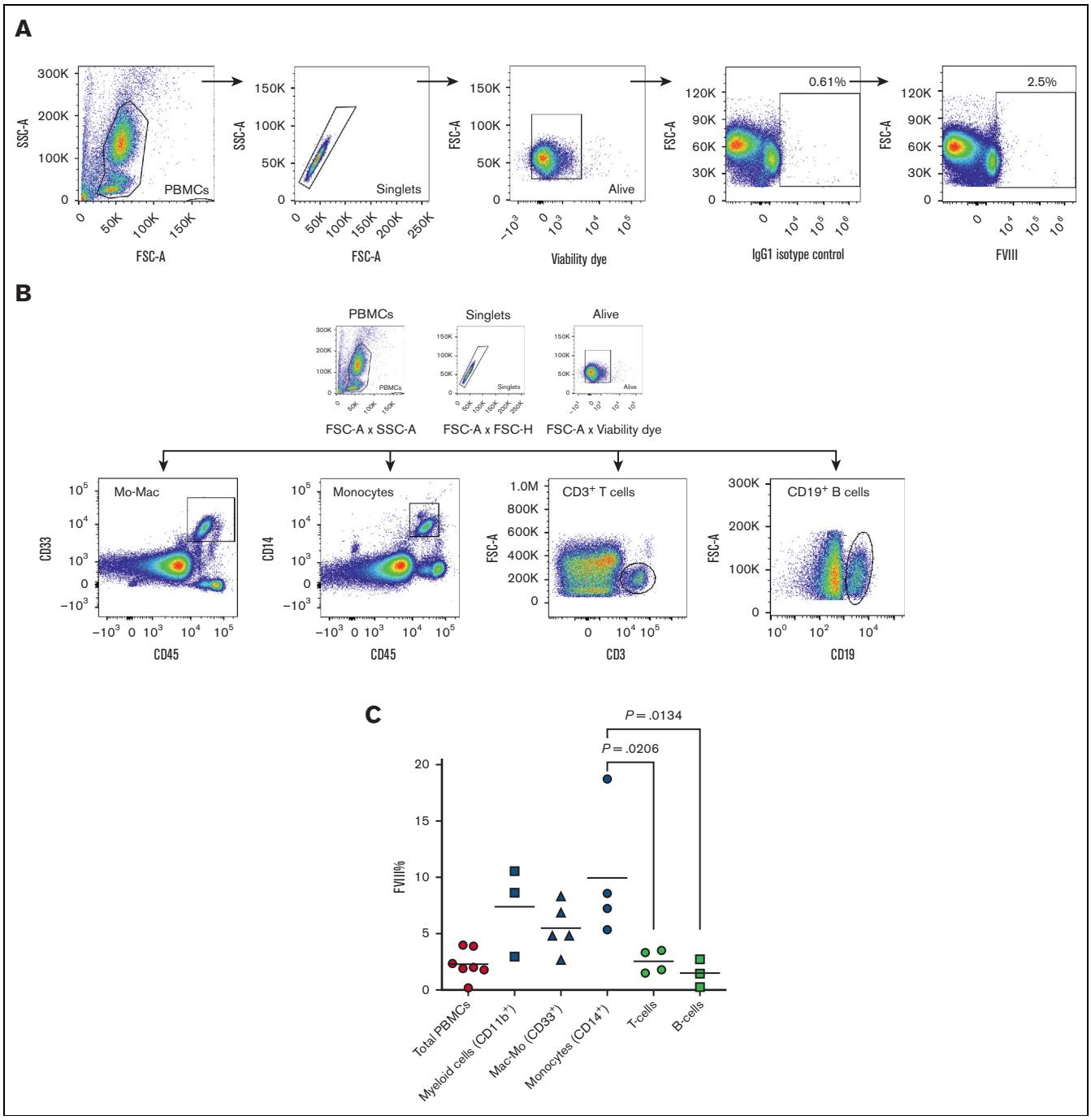

Figure 2. PBMC myeloid compartment is the richest in FVIII$^+$ cells in the hematopoietic system. (A) This logical gating strategy was consistently used to analyze FVIII expression in all samples, with gates on PBMCs, singlets, viable cells, and FVIII vs matched isotype control; here, an example of FVIII percentage in total PBMCs. (B) Gating strategy used for selecting PBMC lymphoid and myeloid subsets. (C) Collective analysis of FVIII expression (%) in different PBMC subsets (n ≥ 3, mean). Mac-Mo, macrophage/monocyte; SSC, side scatter.

same cell population was enriched after 7 to 10 days of culture with the regular HSC-cytokine medium + UM171 (Figure 4D), confirming that UM171 expanded the same cell fraction driven by the endothelial culture. Such cells were optimally transduced by the FVIII transgene in the presence of UM171 and retained transgene expression in 27.5% ± 5.9 of cells after 14 days of e-LTC (P = .007) (Figure 4C, middle and right panels). Taken together, these results show sustained expression of the FVIII transgene in mature CD34–derived monocytes and an expansion of a CD14$^+$/CD31$^+$ cell subpopulation with an excellent capacity for stable expression of the FVIII transgene over time, induced either by UM171 or potentiated by the endothelial culture medium.

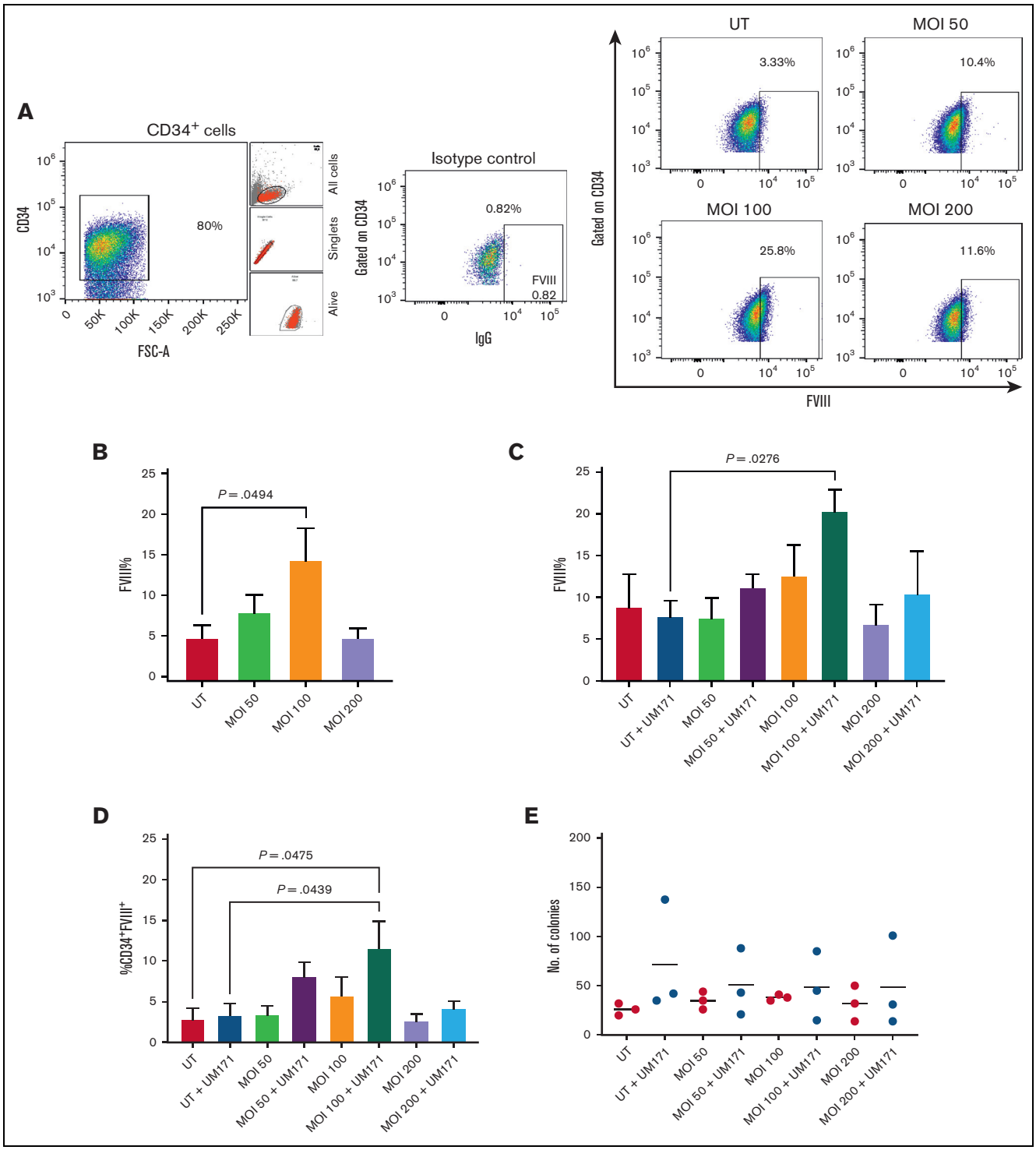

Figure 3. UM171 enhances CD34$^+$ transduction efficiency with FVIII. (A) FC analysis of FVIII overexpression in CD34$^+$ cells transduced with LV-hPGK-hBDDFVIII. Representative FC plots are shown on the right at 50, 100, and 200 MOI. On the left, the gating strategy on CD34$^+$ cells and the IgG isotype control for FVIII staining are displayed. (B) Collective analysis of FVIII expression in CD34$^+$ cells transduced with LV-hPGK-hBDDFVIII (n = 5, mean ± standard error the mean [SEM]). (C) FVIII expression in total CD34$^+$ cells after 7 to 10 days of culture or transduction at different MOI with or without 38 nM UM171 (added every 2 days) (n ≥ 5, mean ± SEM). (D) Rate of FVIII$^+$/CD34$^+$ cells, calculated by multiplying FVIII percentage and CD34 percentage as per the following equation (percentage of FVIII × percentage of CD34$^+$ cells) per 100 (mean ± SEM, n > 5). (E) CD34$^+$ CFU colonies after 14 days (n = 3, mean). UT, untransduced.

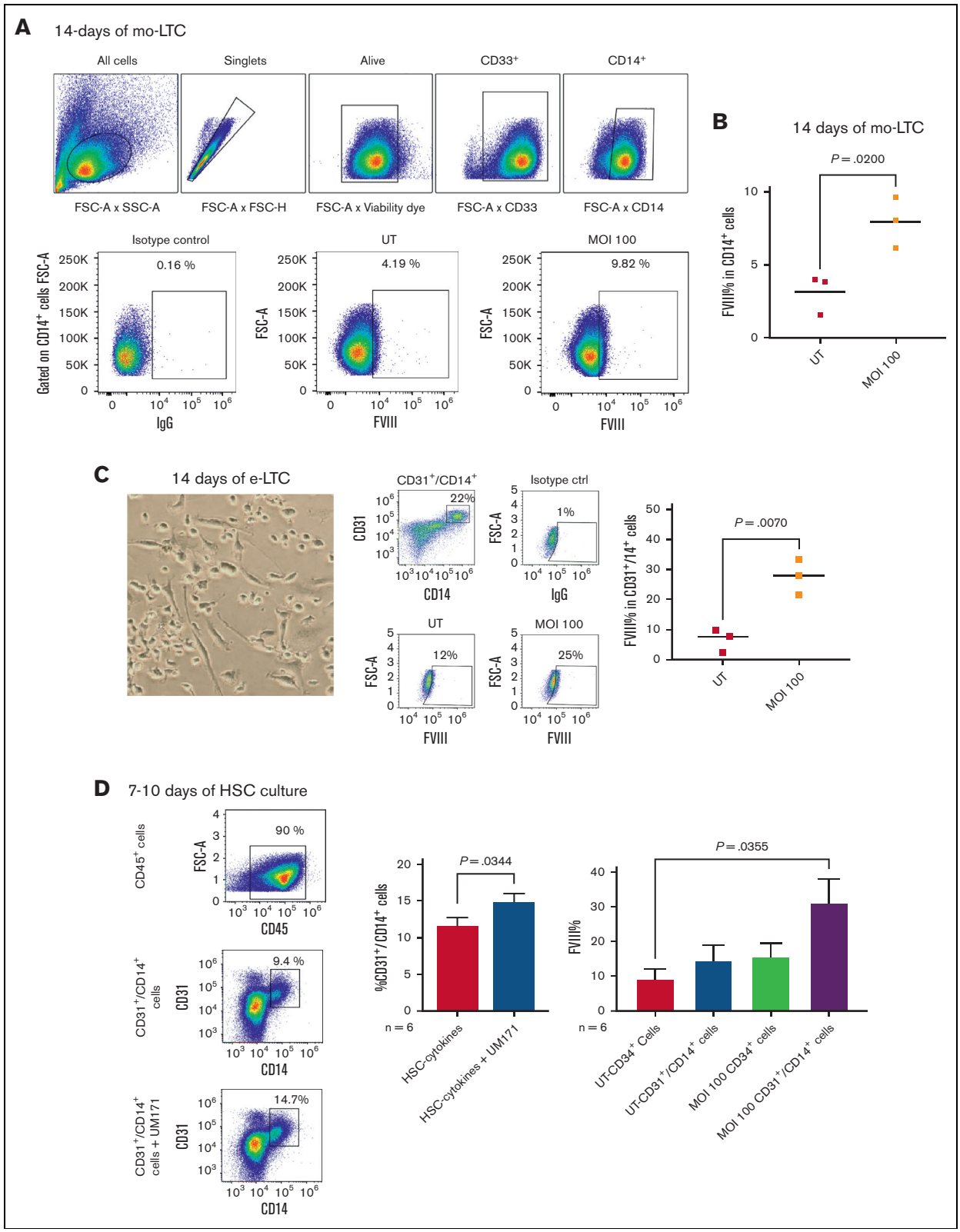

Figure 4. UM171 enriches CD14$^+$/CD31$^+$ monocyte subset with high FVIII expression capacity. (A-B) FVIII expression in CD14$^+$ monocytes differentiated from CD34$^+$ cells after 14 days of monocyte-LTC (mo-LTC) assay. (A) An example of transduction efficiency and logical gating strategy for UT vs 100 MOI transduced CD34$^+$ cells differentiated into CD14$^+$ cells. (B) Collective analysis of FVIII expression in CD14$^+$ monocytes differentiated from UT and transduced CD34$^+$ cells after 14 days of mo-LTC assay (n = 3, mean). (C) A phase-contrast image (original magnification ×20) of adherence, elongation, and cell features after 7 days of the e-LTC assay (left); examples of total

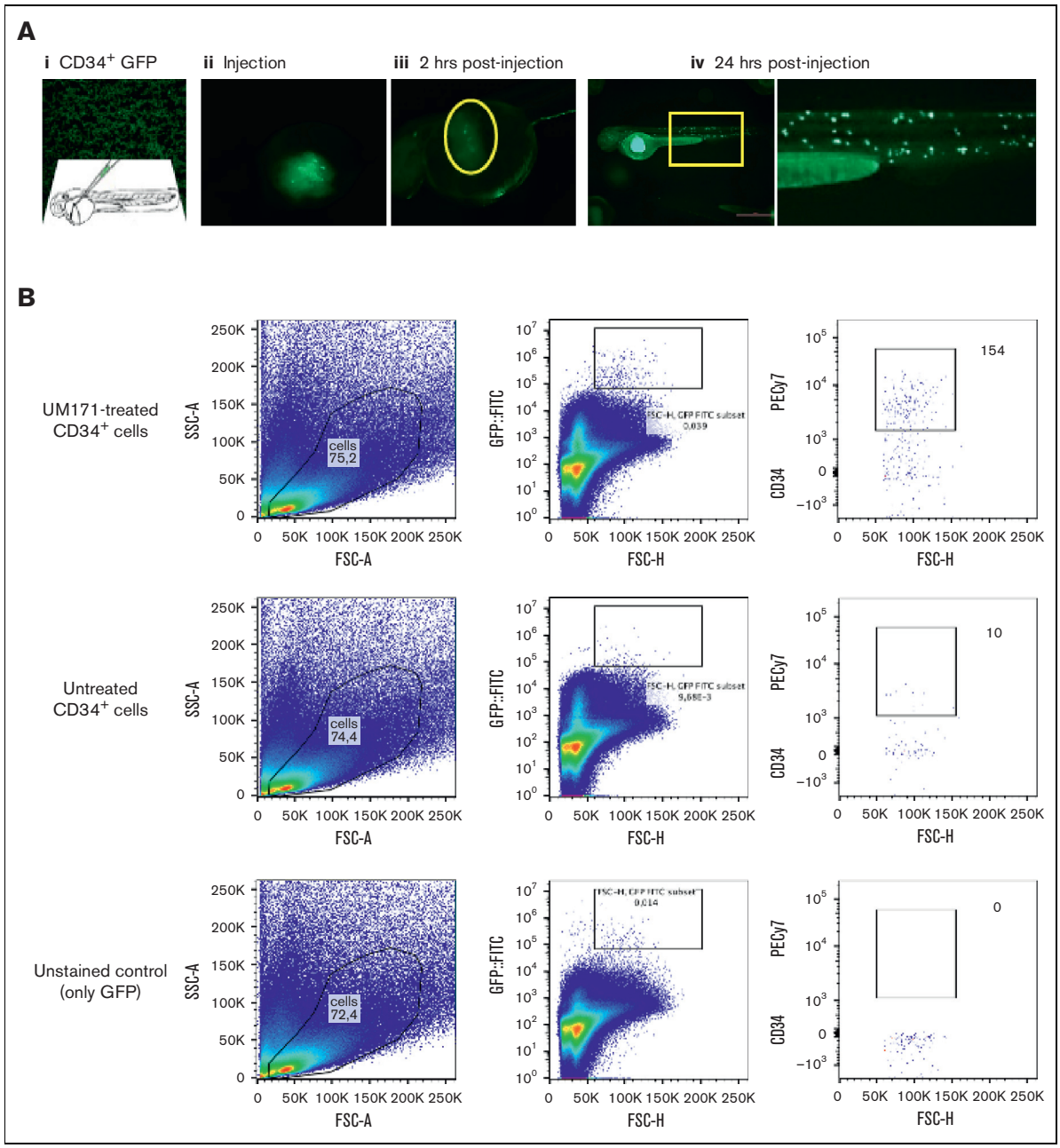

Figure 5. Engraftment and expansion of human CD34$^+$ cells in ZF model. (A) Phases of xenotransplantation of human CD34$^+$ cells transduced with LV-h-PGK-GFP and injected into ZF larvae (the AB wild-type line), slide smear of fluorescent CD34$^+$ (AI), cells at injection site (yolk) (AII), 2 hours postinjection (AIII), and engraftment of cells at 24 hours after injection (AIV). (B) FC logical gating analysis of LV-h-PGK-GFP–transduced CD34$^+$ cells in dissociated ZF larvae injected with UM171-treated and untreated cells (gates indicate the final number of cells). (C) Fluorescence images showing UM171-treated/untreated human CD34$^+$ cells, transduced with rLV.EF1.tdTomato-9 (red), residing in the hematopoietic niche of Tg(fli1:EGFP) ZF (green), (I-III) UM171-treated (AIV-VI). (D) Danioscope analysis of cell mass size in UM171-treated and untreated CD34$^+$ cells (n = 11, mean ± SEM). FITC, fluorescein; GFP, green fluorescence protein.

Figure 4 (continued) CD45$^+$/CD14$^+$/CD31$^+$ cells after 14 days of the e-LTC assay, and FVIII expression in the same cells derived from UT and MOI 100 transduced CD34$^+$ cells (middle); and cumulative expression of FVIII in CD45$^+$/CD14$^+$/CD31$^+$ cells after e-LTC assay (n = 3, mean) (right). (D) FC plots and cumulative data showing CD45$^+$/CD14$^+$/CD31$^+$ enrichment after 10 days of the CD34$^+$ culture in HSC-cytokine medium with or without UM171 (n = 6, mean ± SEM) (left and middle). FVIII expression in transduced and UT CD34$^+$ cells and differentiated CD14$^+$/CD31$^+$ cells after 7 to 10 days culture with UM171 (n = 6, mean ± SEM) (right). e-LTC, endothelial-long term culture; FC, flow cytometry; mo-LTC, monocyte-long term culture.

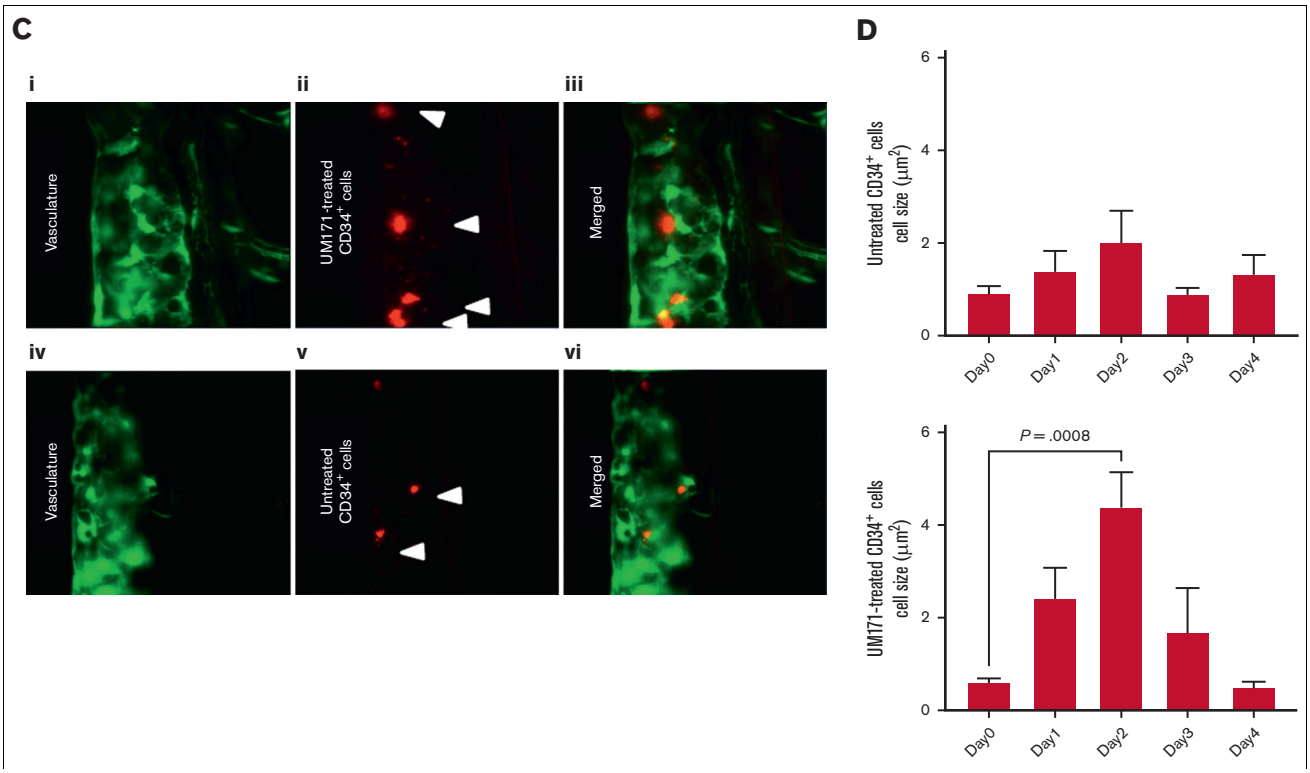

Figure 5 (continued)

Engraftment and expansion of human CD34$^+$ cells in the ZF model

At 24 hours after fertilization, ZF larvae display primitive blood circulation, and at 36 hours after fertilization, definitive HSCs are formed in the ventral wall of the DA. Subsequently, these HSCs migrate to the caudal hematopoietic tissue in the posterior tail area.[30,31] Notably, the ZF model tolerates xenotransplantation without the need for conditioned immunosuppression if it is performed within the first 2 days of the larval stage.

Human CD34$^+$ cells were successfully engrafted into 24 hours after fertilization ZF embryos and, after 1 day after injection, appeared to circulate in the vasculature and reside in the caudal niche (Figure 5A). The addition of UM171 to the CD34$^+$ cell culture displayed an average of a twofold increase in expansion, peaking at day 2 after xenotransplantation ($P = .0008$) (Figure 5B-D; supplemental Figure 1; supplemental Video 1).

HA ZF modeling with f8-MO antisense RNA

After evaluating the ability of the UM171-treated cells to engraft and proliferate in vivo, we modeled the transient HA phenotype in the ZF by injecting antisense f8-MO. To map the content and distribution of F8 in the fish, we used a fluorescent f8-MO molecule, which allows for visualizing the binding moiety of *f8* RNA in vivo. Surprisingly, after injecting f8-MO at the 1-cell stage and visualizing the larvae on day 3 (72 hours after fertilization), the fluorescent antisense f8 was predominantly located in the hematopoietic area and DA (Figure 6A; supplemental Video 2), suggesting that F8 plays a functional role in the hematopoietic system of ZF, as previously described.[32]

The effect of progressive f8-MO doses (0.5-1.25 mM) on ZF survival and clot formation was subsequently evaluated. Higher doses of 1.0 and 1.25 mM negatively affected ZF survival (Figure 6B). Interestingly, during the screening of the f8-MO group phenotype, we noticed that these larvae had significantly lower blood flow. Quantitative analysis revealed that blood flow activity (percentage of circulating blood cells measured in the selected area of the vessels, DA and PCV) was significantly reduced in the f8-MO treatment (0.75-1.25 mM) groups compared with the control (Figure 6C; supplemental Video 3). This result corroborates the hypothesis that FVIII promotes hematopoiesis. Furthermore, the assessment of clot formation time upon delivering laser injury to the PCV showed that all concentrations of f8-MO significantly impaired the clot formation, with a trending peak at a dose of 1 mM compared with the control (Figure 6D).

After obtaining the HA phenotype, we assessed the feasibility of injecting human cells through a needle into the duct of Cuvier at 48 hours after fertilization in f8-MO knockdowns (Figure 5A). Unfortunately, cell injection attempts led to uncontrolled bleeding in f8-MO–treated ZF and a further decrease in blood volume, which severely impaired the survival after laser injury and prevented us from using this model to study cell-mediated correction of HA.

To overcome this obstacle and assess the contribution of human CD34$^+$ cells to the rescue of the HA phenotype in ZF, we coinjected f8-MO with human cells into the duct of Cuvier at 48 hours after fertilization. This method ensured the safe homing of cells in hematopoietic areas and enabled wound clotting before MO exerts an inhibitory effect on coagulation, which is expected ~30 minutes after injection. This method efficiently allowed us to test our

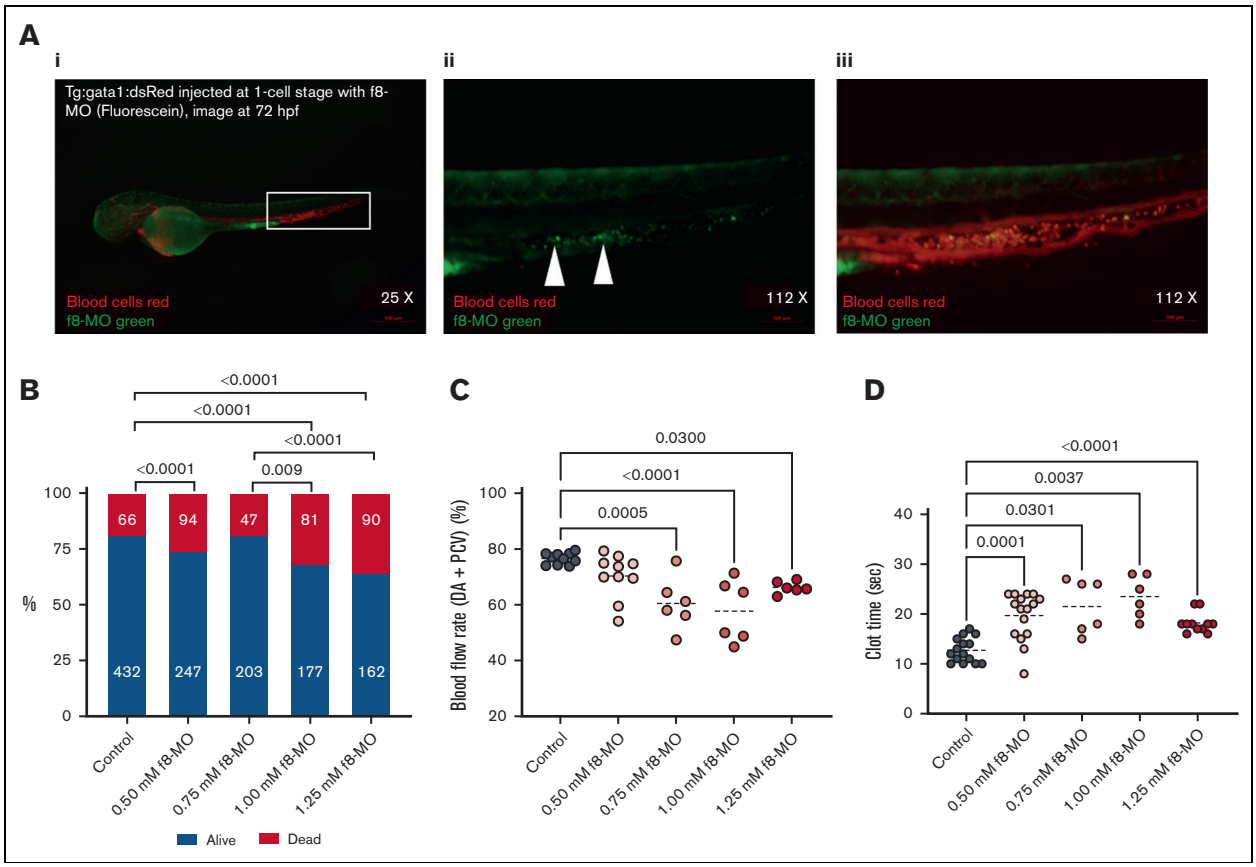

Figure 6. HA ZF modeling with f8-MO antisense RNA. (A) Representative fluorescence images: (I) merged and zoomed-in image of Tg:gata1:dsRed ZF larvae, injected with 1.0 mM f8-MO and tagged with fluorescein at 1-cell stage and visualized at 72 hours after fertilization. The hematopoietic niche is contoured by a white box (×25 magnification); (II) Green fluorescence zoomed in image of f8-MO localized in the hematopoietic niche as shown by the arrows (original magnification ×112); and (III) Merged image (original magnification ×112) showing transgenic red blood cells (red) and f8-MO (green, merged = orange). (B) Viability percentage of ZF larvae injected with f8-MO. The number of measured ZF is noted on the columns. Significance was calculated on a χ^2 test, with a subsequent pairwise post hoc z test (C) Danioscope calculation of the blood flow activity in selected areas of the DA and PCV. The average DA plus PCV blood flow activity (%) of all MO groups was compared with the control group ($n \geq 6$, mean). (D) Laser-induced injury and clot formation time of ZF injected with f8-MO ($n \geq 6$, mean).

hypothesis in vivo, and all HA-related xenotransplantation results in this study refer to this optimized f8-MO knockdown model.

UM171-treated CD34$^+$ reduce clot formation time in wild-type ZF

To assess the baseline FVIII expression in the UM171-treated CD34$^+$, we first injected normal larvae with CD34$^+$ cells at 48 hours after fertilization. Subsequently, we performed a laser-mediated endothelial injury in the CVP region at 1 and 2 days after injection. UM171-treated CD34$^+$ cells displayed a significantly reduced clot formation time compared with the control ZF, with a greater difference measured at 1 day after injection (Figure 7A; supplemental Video 4).

To dissect the contribution of CD34$^+$ cells and UM171 treatment in reducing the clot formation, adjusting for the advantage in engraftment granted by UM171, we injected 2 groups of ZF with an equal number of UM171-treated and nontreated CD34$^+$ cells at 48 hours after fertilization, and we analyzed the clotting time at 1 and 3 days after injection. UM171 treatment of CD34$^+$ cells triggered an independent significant reduction of clot time after laser injury. This effect was stable over time because the differences were maintained at 3 days after injection, when the hematopoiesis is definitive in ZF (Figure 7B).

UM171-FVIII–transduced CD34$^+$ progeny rescues the HA ZF

Our in vitro experiments showed that CD34-derived CD14$^+$/CD31$^+$ cells were the richest carriers of FVIII among all mature white blood cells. Therefore, we directly tested the ability of this progeny to secrete functional FVIII in vivo. Specifically, we caused an overexpression of FVIII in CD34$^+$ cells via LV transduction, and after 7 days of UM171 expansion, we sorted the CD14$^+$/CD31$^+$ fraction and transferred it to HA ZF. We repeated the clot formation analyses on days 1 and 6 after the injection, which represents the longest analyzable time point before the disappearance of the MO effect.

On day 1, the UM171-FVIII CD14$^+$/CD31$^+$ transduced cells reduced the clot formation time in HA ZF from 24.3 (±6.2) seconds to 8.9 (±1.8) seconds, compared with 15 (±2.5) seconds in the untransduced CD14$^+$/CD31$^+$ condition (Figure 7C). These results

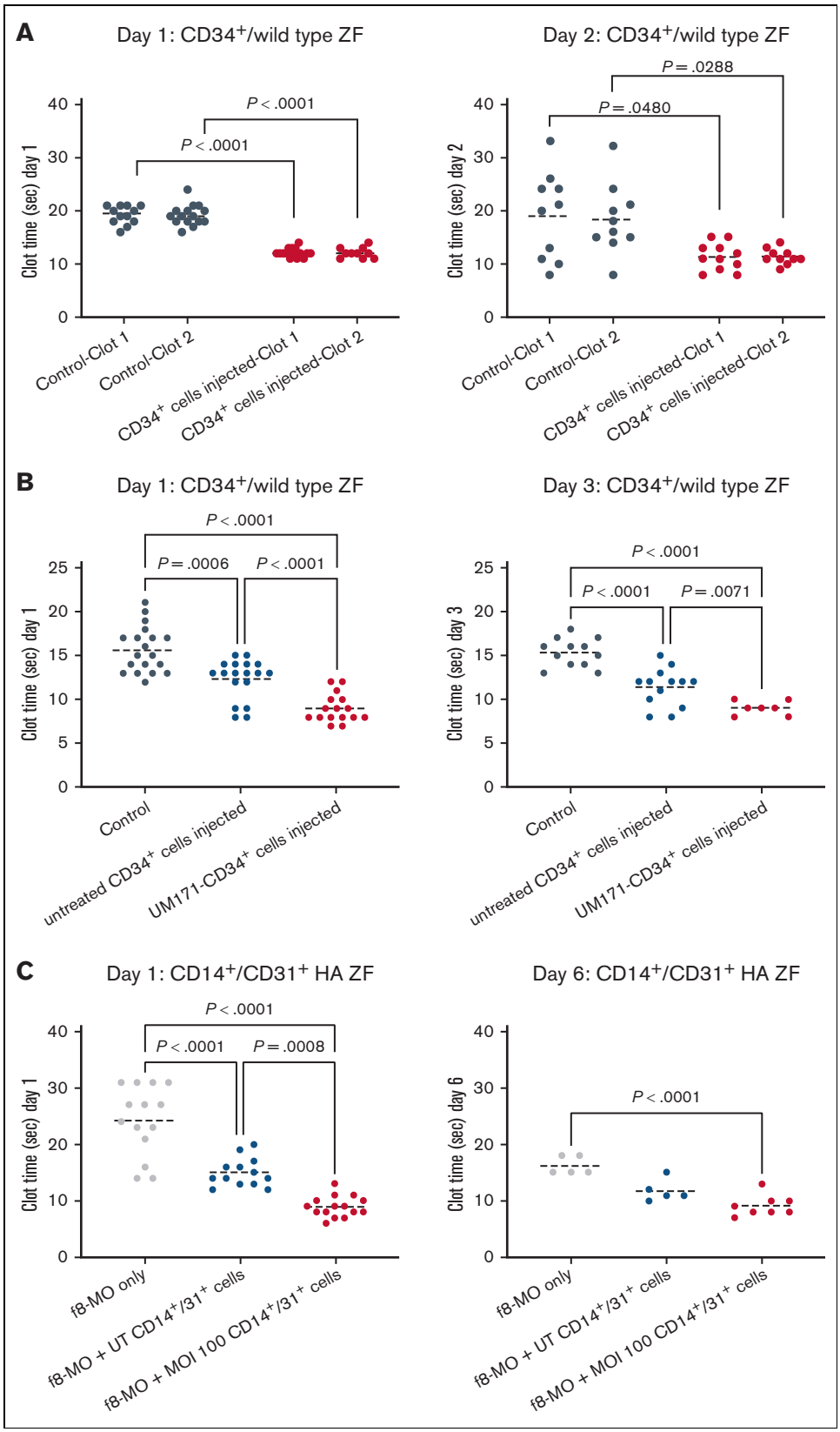

Figure 7. Cell-mediated rescuing of HA phenotype in ZF model. (A) Clot formation times in laser-injured ZF (injuries are performed in duplicate and consequently in 2 sites of the CVP region) injected with human CD34$^+$ cells and injured at day 1 (left) and day 2 (right) after injection (n ≥ 10, mean). (B) Clot formation time in laser-injured ZF injected with UM171-treated (red dots) and untreated (blue dots) sorted human CD34$^+$ cells at days 1 and 3 after injection (n ≥ 7, mean). (C) Clot formation time in laser-injured HA ZF treated

show that transduced CD34-derived $CD14^+/CD31^+$ cells have a high capacity to secrete functional FVIII and correct HA defects. The production of the FVIII transgene was also examined on day 6 after injection. There was a significant reduction in the clot formation time in HA ZF with the xenotransplantation of transduced $CD14^+/CD31^+$ cells compared with the control HA group without xenotransplantation. This indicates a long-term functional secretion of the FVIII transgene. Taken together, these data demonstrate that $CD14^+/CD31^+$ monocytes derived from UM171-treated transduced $CD34^+$ cells can fully express the FVIII transgene and correct the bleeding tendency in the f8-MO knockdown ZF model of HA.

Discussion

LV transduction of HSCs for the correction of HA has been proven effective in mouse models, with the FVIII transgene directed to megakaryocytes[8] and CD68 monocytes/macrophages[10] through specific promoters. Clinical trials have recently started to offer HSC-targeting GT options to patients with HA after the successful completion of the preclinical project phase,[5] thus, paving the way for HSC-directed HA GT. In this study, the most suitable $CD34^+$ cell lineage to carry functional FVIII was carefully evaluated. This screening was made possible because of an in-house optimized FC method for visualizing intracellular FVIII.[14] This method has proven to be excellent for measuring FVIII content in blood cells, opening the possibility of a practical and patient-tailored readout for ongoing GT trials.

Among white blood cells, the mature myeloid cell lineage was the richest in FVIII. Within this lineage, $CD14^+/CD31^+$ monocytes proved to be suitable carriers of FVIII, expressing the highest rate of natural and transgenic LV-mediated FVIII in short- and long-term cultures. Endothelium is a natural source of FVIII in the human body[27] and $CD14^+/CD31^+$ cells are exciting targets for FVIII GT because of the fact that they share endothelial properties. The potential of $CD34^+$ cells to differentiate into endothelium is disputed in literature, and the rarity of $CD34^+$ cell progenitors confounds a clear understanding of this phenomenon.[33] Although many studies tried to determine which blood progenitor can give rise to endothelial cells,[34,35] other studies support the hypothesis that cells are characterized by mature lineage infidelity rather than progenitor plasticity.[36] For instance, monocytes are capable of acquiring endothelial phenotype and function under certain pathophysiological conditions.[37] This phenomenon is also observed for other cell types, especially during wound repair.[36] Interestingly, it is proposed that $CD14^+/CD31^+$ cells endow a cell population of so-called "monocyte-derived endothelial progenitors,"[38] which do not generate mature endothelium but rather migrate to the vessels in the event of injury, contributing to endothelial repair, angiogenesis, and neovascularization through the release of cytokines.[39,40]

The presence of an FVIII reservoir in proximity to endothelial sites can be of great advantage in triggering immediate hemostasis in patients with HA. Moreover, an HSC source of FVIII GT-corrected mature cells would ensure continuous renewal of this cell population.

To assess the potential of FVIII-transduced $CD34^+$ cells for in vivo GT, we chose the ZF model, which has several advantages over larger animal models, such as rapid development and adequate transparency to perform live whole-animal imaging. Indeed, ZF has notable advantages for studying hematopoiesis specifically,[41,42] and it has successfully been used in previous studies to describe coagulation defects, including those associated with FVII, von Willebrand factor, fibrinogen,[43] and FV.[20] Using this model, we discovered that FVIII is a key coagulation factor in ZF, and it has extracoagulative effects, likely at the stem cell level, supporting blood circulation in the fish. Previous research in mice described a key role of FVIII in maintaining the long-term repopulating HSC compartment through FVIII/thrombin/protease-activated receptor 1 (PAR1) in an HSC stromal axis.[32] The high concentration of *f8* RNA in the hematopoietic system of 48-hours postfertilization larvae adds evidence for a functional role of FVIII in hematopoiesis. Although at this point we cannot better clarify this mechanism, the strong impact of FVIII on ZF blood output warrants further investigation in this direction.

When we evaluated whether xenotransplanted HSCs had any baseline effect on coagulation in normal ZF, we found that the $CD34^+$ cell progeny reduced the clot formation time after laser-mediated injury. This effect might be attributed to several reasons. For instance, because $CD34^+$ cytokine activation in vitro increased FVIII expression 10-fold, similarly, their engraftment activity in vivo might provide an increase in FVIII availability. Conversely, this effect might be granted by CD34-derived lineages; besides $CD14^+/CD31^+$ monocytes, megakaryocytes might also increase the pool of available platelets in fish, especially within the first 48 hours after fertilization when fish hematopoiesis is still predominantly transient.

Treating HSCs with UM171 further contributed to reducing clot formation time because of a still unexplained qualitative effect on xenotransplanted cells. UM171 is a clinical-grade compound with stem cell enhancing properties, known to upregulate the endothelial protein C receptor (EPCR)/PAR1 molecule on HSCs. EPCR/PAR1 activates reactive oxygen species detoxification programs in HSCs,[44] thus, enhancing EPCR/PAR1 on $CD34^+$ cells may help the development of healthier progenitors for producing mature cells with a possible role in coagulation. EPCR/PAR1 receptor also acts as a key mediator in thrombin-induced platelet activation.[45] Considering our observations, together with the previously published work in mice,[32] we can speculate that the same FVIII/thrombin/PAR1 pathway could both act on HSC pool maintenance and accelerate the clotting process. More in-depth studies are needed to clarify this hypothesis and the effects of FVIII on hematopoiesis.

Finally, we successfully created a transient HA ZF model in 2-day-old larvae by blocking FVIII with *f8*-MO RNA interference. We used the only possible time window to ensure the safe homing of human transplanted cells while reducing bleeding in the HA ZF for a proper readout. With this model, we showed that $CD14^+/CD31^+$ monocytes derived from FVIII-transduced $CD34^+$ cells could rescue the coagulation defect in fish up to 6 days after

Figure 7 (continued) with 1.00 mM f8-MO only (gray dots) and injected with either sorted UT $CD14^+/CD31^+$ cells (blue dots) or sorted cells transduced with LV-hPGK-hBDDFVIII (red dots). Both UT and transduced cells were treated with UM171. Measurements were acquired on days 1 and 6 after injection ($n \geq 5$, mean).

xenotransplantation, which represents the longest time that can be examined in MO transient interference. This result implies the ability of transduced $CD14^+/CD31^+$ monocytes to secrete long-term functional FVIII protein, improving the effect granted by UM171 treatment only.

In this study, we did not address any possible harmful consequences on LV-FVIII integration in HSC, including insertional mutagenesis, or enhanced immunogenicity of FVIII expression in the context of the hematopoietic system. Rather, we intended this work as a proof-of-concept selection of an optimal GT target blood cell type, based on a systematic screening.

Despite the preliminary nature of this work, to facilitate a future clinical translation, we used clinically tested transduction and expansion protocols, and we purposely chose CB as HSC source to propose it as an alternative FVIII GT source. Such a source would mitigate unnecessary bleeding risks associated with collecting HSC from bone marrow or peripheral blood for autologous transplantation in susceptible patients with HA. If diagnosed prenatally, newborns affected by familial HA could potentially benefit from CB banking and FVIII GT correction after UM171 cell expansion. After proper safety evaluations, the powerful expansion ability of UM171 CB[22,23] could be used to further optimize the GT procedure with multiple transductions and obtain clinically adequate batches of FVIII GT-carrying CB stem cells to be used for single or repeated infusions.

In conclusion, we measured the intracellular content of FVIII in HSCs and mature PBMCs and identified UM171-expanded $CD14^+/CD31^+$ monocytes as the most suitable cell lineage for carrying FVIII. Such cells rescued the ZF HA model, serving as an adequate source of FVIII in the event of vascular injury. While the successful FC-based FVIII detection method and the novel ZF model could be useful for any prospective HA studies, our findings in the HA ZF open up opportunities to explore the use of UM171-expanded $CD34^+$ cells for HA GT, after LV transduction with a specific promoter able to induce FVIII expression in $CD14^+/CD31^+$ cells.

Acknowledgments

The authors thank Gürkan Mollaoğlu from Mount Sinai Hematology and Medical Oncology Division NY and Ilya Demchenko from Insight Editing London for revising the manuscript.

This work was supported by Sidra Medicine research internal funding (S. Deola and C.C.) and grants from Telethon (grant GGP19201) (A.F.) and Fondazione Cariplo (grant 2018-0253) (C.B.).

Authorship

Contribution: S. Deola and A.F. conceived the study, planned experiments, and analyzed data; S. Deola coordinated and supervised the project and wrote the manuscript; M.E., A.A.-M., W.H., and J.-C.G. planned and performed experiments; D.A., M.J.A.-K., G.G., I.P., A.S., and D.K. performed experiments; A.I.A. and C.B. planned research and revised the manuscript; S.M. and D.O. procured cord blood specimens and discussed experiments; C.C. planned research; and S. Da'as planned research, performed experiments, and revised the manuscript.

Conflict-of-interest disclosure: The authors declare no competing financial interests.

ORCID profiles: W.H., 0000-0003-1219-2671; D.A., 0000-0002-8434-3566; G.G., 0000-0003-3546-8642; A.I.A., 0000-0003-0688-5578; C.C., 0000-0002-1664-3030; C.B., 0000-0001-9704-0647; A.F., 0000-0001-9780-300X; S. Da'as, 0000-0003-3438-5028; S. Deola, 0000-0002-3178-1271.

Correspondence: Sara Deola, Sidra Medicine, Research, Advanced Cell Therapy Core, Al Luqta St, Doha, Qatar; email: sdeola@sidra.org.

References

1. Rangarajan S, Walsh L, Lester W, et al. AAV5-factor VIII gene transfer in severe hemophilia A. *N Engl J Med*. 2017;377(26):2519-2530.
2. Regling K, Callaghan MU, Sidonio R. Managing severe hemophilia a in children: pharmacotherapeutic options. *Pediatr Health Med Therapeut*. 2022;13:27-35.
3. Monahan PE, Négrier C, Tarantino M, Valentino LA, Mingozzi F. Emerging immunogenicity and genotoxicity considerations of adeno-associated virus vector gene therapy for hemophilia. *J Clin Monit*. 2021;10(11):2471-2494.
4. Poothong J, Pottekat A, Siirin M, et al. Factor VIII exhibits chaperone-dependent and glucose-regulated reversible amyloid formation in the endoplasmic reticulum. *Blood*. 2020;135(21):1899-1911.
5. Batty P, Lillicrap D. Hemophilia gene therapy: approaching the first licensed product. *Hemasphere*. 2021;5(3):e540.
6. Follenzi A, Raut S, Merlin S, Sarkar R, Gupta S. Role of bone marrow transplantation for correcting hemophilia A in mice. *Blood*. 2012;119(23):5532-5542.
7. Miao CH. Hemophilia A gene therapy via intraosseous delivery of factor VIII-lentiviral vectors. *Thromb J*. 2016;14(suppl 1):41, 93-99.
8. Chen J, Schroeder JA, Luo X, Montgomery RR, Shi Q. The impact of GPIbα on platelet-targeted FVIII gene therapy in hemophilia A mice with pre-existing anti-FVIII immunity. *J Thromb Haemostasis*. 2019;17(3):449-459.
9. Zanolini D, Merlin S, Feola M, et al. Extrahepatic sources of factor VIII potentially contribute to the coagulation cascade correcting the bleeding phenotype of mice with hemophilia A. *Haematologica*. 2015;100(7):881-892.
10. Doering CB, Denning G, Shields JE, et al. Preclinical development of a hematopoietic stem and progenitor cell bioengineered factor VIII lentiviral vector gene therapy for hemophilia A. *Hum Gene Ther*. 2018;29(10):1183-1201.

11. Porada CD, Sanada C, Kuo C-J, et al. Phenotypic correction of hemophilia A in sheep by postnatal intraperitoneal transplantation of FVIII-expressing MSC. *Exp Hematol*. 2011;39(12):1124-1135.e4.
12. Aiuti A, Biasco L, Scaramuzza S, et al. Lentiviral hematopoietic stem cell gene therapy in patients with Wiskott-Aldrich syndrome. *Science*. 2013; 341(6148):1233151-12.
13. Olgasi C, Borsotti C, Merlin S, et al. Efficient and safe correction of hemophilia A by lentiviral vector-transduced BOECs in an implantable device. *Mol Ther Methods Clin Dev*. 2021;23:551-566.
14. Elnaggar M, Al-Mohannadi A, Kizhakayil D, et al. Flow-cytometry platform for intracellular detection of FVIII in blood cells: a new tool to assess gene therapy efficiency for hemophilia A. *Mol Ther Methods Clin Dev*. 2020;17:1-12.
15. Stec M, Weglarczyk K, Baran J, et al. Expansion and differentiation of $CD14^{+}CD16^{-}$ and $CD14^{++}CD16^{+}$ human monocyte subsets from cord blood $CD34^{+}$ hematopoietic progenitors. *J Leukoc Biol*. 2007;82(3):594-602.
16. Gehling UM, Ergün S, Schumacher U, et al. In vitro differentiation of endothelial cells from AC133-positive progenitor cells. *Blood*. 2000;95(10): 3106-3112.
17. Cabezas-Sainz P, Guerra-Varela J, Carreira MJ, et al. Improving zebrafish embryo xenotransplantation conditions by increasing incubation temperature and establishing a proliferation index with ZFtool. *BMC Cancer*. 2018;18(1):3.
18. Bresciani E, Broadbridge E, Liu PP. An efficient dissociation protocol for generation of single cell suspension from zebrafish embryos and larvae. *MethodsX*. 2018;5:1287-1290.
19. Da'as SI, Aamer W, Hasan W, et al. PGAP3 associated with hyperphosphatasia with mental retardation plays a novel role in brain morphogenesis and neuronal wiring at early development. *Cells*. 2020;9(8):E1782.
20. Weyand AC, Grzegorski SJ, Rost MS, et al. Analysis of factor V in zebrafish demonstrates minimal levels needed for early hemostasis. *Blood Adv*. 2019; 3(11):1670-1680.
21. Fares I, Chagraoui J, Gareau Y, et al. Cord blood expansion. Pyrimidoindole derivatives are agonists of human hematopoietic stem cell self-renewal. *Science*. 2014;345(6203):1509-1512.
22. Cohen S, Roy J, Lachance S, et al. Hematopoietic stem cell transplantation using single UM171-expanded cord blood: a single-arm, phase 1-2 safety and feasibility study. *Lancet Haematol*. 2020;7(2):e134-e145.
23. Dumont-Lagacé M, Li Q, Tanguay M, et al. UM171-expanded cord blood transplants support robust T Cell reconstitution with low rates of severe infections. *Transplant Cell Ther*. 2021;27(1):76.e1-76.e9.
24. Lin Y, Weisdorf DJ, Solovey A, Hebbel RP. Origins of circulating endothelial cells and endothelial outgrowth from blood. *J Clin Invest*. 2000;105(1): 71-77.
25. Rohde E, Malischnik C, Thaler D, et al. Blood monocytes mimic endothelial progenitor cells. *Stem Cell*. 2006;24(2):357-367.
26. Schmeisser A. Monocytes coexpress endothelial and macrophagocytic lineage markers and form cord-like structures in Matrigel under angiogenic conditions. *Cardiovasc Res*. 2001;49(3):671-680.
27. Turner NA, Moake JL. Factor VIII is synthesized in human endothelial cells, packaged in Weibel-Palade bodies and secreted bound to ULVWF strings. *PLoS One*. 2015;10(10):e0140740.
28. Sun J-H, Zhang Y-L, Nie C-H, et al. In vitro labeling of endothelial progenitor cells isolated from peripheral blood with superparamagnetic iron oxide nanoparticles. *Mol Med Rep*. 2012;6(2):282-286.
29. Woodfin A, Voisin M-B, Nourshargh S. PECAM-1: a multi-functional molecule in inflammation and vascular biology. *Arterioscler Thromb Vasc Biol*. 2007;27(12):2514-2523.
30. Sugden WW, North TE. Making blood from the vessel: extrinsic and environmental cues guiding the endothelial-to-hematopoietic transition. *Life*. 2021; 11(10):1027-1048.
31. Boatman S, Barrett F, Satishchandran S, et al. Assaying hematopoiesis using zebrafish. *Blood Cells Mol Dis*. 2013;51(4):271-276.
32. Aronovich A, Nur Y, Shezen E, et al. A novel role for factor VIII and thrombin/PAR1 in regulating hematopoiesis and its interplay with the bone structure. *Blood*. 2013;122(15):2562-2571.
33. Rafii S. Circulating endothelial precursors: mystery, reality, and promise. *J Clin Invest*. 2000;105(1):17-19.
34. Peichev M, Naiyer AJ, Pereira D, et al. Expression of VEGFR-2 and AC133 by circulating human CD34(+) cells identifies a population of functional endothelial precursors. *Blood*. 2000;95(3):952-958.
35. Safi W, Kuehnl A, Nüssler A, Eckstein H-H, Pelisek J. Differentiation of human $CD14^{+}$ monocytes: an experimental investigation of the optimal culture medium and evidence of a lack of differentiation along the endothelial line. *Exp Mol Med*. 2016;48(4):e227-e235.
36. Ge Y, Gomez NC, Adam RC, et al. Stem cell lineage infidelity drives wound repair and cancer. *Cell*. 2017;169(4):636-650.e14.
37. Kim S-J, Kim J-S, Papadopoulos J, et al. Circulating monocytes expressing CD31. *Am J Pathol*. 2009;174(5):1972-1980.
38. Rehman J, Li J, Orschell CM, March KL. Peripheral blood "endothelial progenitor cells" are derived from monocyte/macrophages and secrete angiogenic growth factors. *Circulation*. 2003;107(8):1164-1169.
39. Shi Q, Rafii S, Wu MH, et al. Evidence for circulating bone marrow-derived endothelial cells. *Blood*. 1998;92(2):362-367.
40. Lopes-Coelho F, Silva F, Gouveia-Fernandes S, et al. Monocytes as endothelial progenitor cells (EPCs), another brick in the wall to disentangle tumor angiogenesis. *Cells*. 2020;9(1):107-133.

41. Carradice D, Lieschke GJ. Zebrafish in hematology: sushi or science? *Blood*. 2008;111(7):3331-3342.

42. Tamplin OJ, Durand EM, Carr LA, et al. Hematopoietic stem cell arrival triggers dynamic remodeling of the perivascular niche. *Cell*. 2015;160(1-2):241-252.

43. Kretz CA, Weyand AC, Shavit JA. Modeling disorders of blood coagulation in the zebrafish. *Curr Pathobiol Rep*. 2015;3(2):155-161.

44. Chagraoui J, Lehnertz B, Girard S, et al. UM171 induces a homeostatic inflammatory-detoxification response supporting human HSC self-renewal. *PLoS One*. 2019;14(11):e0224900-e0224916.

45. Andersen H, Greenberg DL, Fujikawa K, et al. Protease-activated receptor 1 is the primary mediator of thrombin-stimulated platelet procoagulant activity. *Proc Natl Acad Sci U S A*. 1999;96(20):11189-11193.